ELSEVIER

Ecological Modelling 141 (2001) 77–103

ECOLOGICAL MODELLING

www.elsevier.com/locate/ecolmodel

Biogeochemical model of Lake Zürich: model equations and results

Martin Omlin [a], Peter Reichert [a,*], Richard Forster [b]

[a] *Swiss Federal Institute for Environmental Science and Technology (EAWAG), CH-8600 Dübendorf, Switzerland*
[b] *Wasserversorgung Zürich, Hardhof 9, CH-8023 Zürich, Switzerland*

Received 14 April 2000; received in revised form 13 December 2000; accepted 9 January 2001

Abstract

A mathematical model for plankton, nutrient (phosphate, ammonia and nitrate) and oxygen dynamics in lakes was developed. It is based on horizontally averaged changes in substance and organism concentrations due to vertical mixing, sedimentation, in- and outflows and biogeochemical conversion processes in the water column and in adjacent sediment layers. The biological part of the model was kept as simple as possible with the three plankton classes *Planktothrix Oscillatoria) rubescens* (most abundant blue-green algae in the lake), other algae and zooplankton. Due to a strong phosphate limitation of algae growth in summer, the stoichiometry of primary production with respect to phosphorus had to be made variable in order to describe data sets available from Lake Zürich. In addition, a process of phosphate uptake of organic particles sinking through the hypolimnion had to be taken into account. After adjusting some model parameters, the model was able to reproduce the key features of the nutrient and oxygen profiles and of algae–zooplankton interactions over several years. However, it was not able to predict occasionally occurring blooms of specific types of algae. This shows that the model is a good tool for studying the dynamics of the key processes governing plankton and nutrient dynamics in the lake, but that it is not detailed enough for the investigation of rarely occurring phenomena involving specific types of algae and for an accurate representation of zooplankton dynamics.

Keywords: Lake Zürich; Water quality modelling; Nutrients; Plankton; Variable stoichiometry; Phosphate uptake

1. Introduction

Water quality of Lake Zürich is of importance for the local water supply authority (Wasserversorgung Zürich, WVZ) because the lake is an important source for drinking water. About 70% of the drinking water in the region of Zürich originates from the lake. This water is used by almost 1 000 000 people.

In order to be able to early recognise problems with raw water quality from Lake Zürich, WVZ conducts a lake water quality monitoring program.

* Corresponding author. Tel.: +41-1-8235281; fax: +41-1-8235375.
E-mail address: reichert@eawag.ch (P. Reichert).

0304-3800/01/$ - see front matter
PII: S0304-3800(01)00256-3

In this paper, a model is described which is designed to quantitatively represent the processes leading to the dynamics of nutrients, oxygen and plankton in the lake. In the present stage, the main purpose of this model is to gain a quantitative understanding of the biogeochemical conversion processes in the lake. However, it is planned to investigate the predictive capabilities of the model in order to extend it to a water quality prediction tool for Lake Zürich that supports the experts in interpreting the data.

This paper is structured as follows. In Section 2, a brief survey is given on Lake Zürich and on the data used for simulation and model calibration. This section is followed by a brief review of published lake water quality models in Section 3. The model used in this paper is described in detail in Section 4 and the results are discussed in Section 5. Finally, the key results with respect to model structure and results are summarized in Section 6. Although the chosen engineering approach simplifies the system to a very high degree and does not include a detailed analysis of the food web, the model still contains a large number of uncertain model parameters. This makes a careful analysis of sensitivity, identifiability, and prediction uncertainty mandatory. This analysis goes beyond the scope of this paper and is delegated to a separate paper (Omlin et al., 2001).

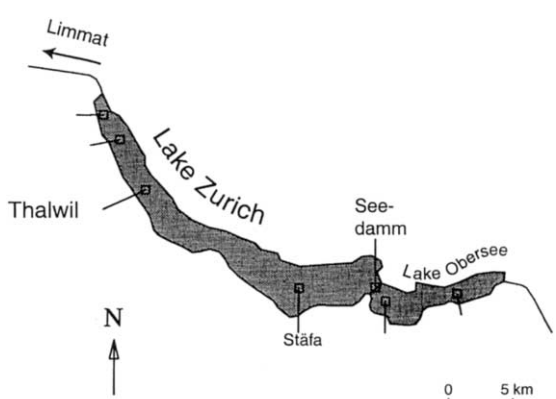

Fig. 1. Lake Zürich with Lake Obersee and the sampling sites of the WVZ water quality monitoring program.

2. Lake Zürich

2.1. Lake description

Located at the border between the midland and the prealpine region of Switzerland Lake Zürich is enclosed by two ridges which protect the lake from direct exposure to the dominant west winds. The basin leads from the upper end at Rapperswil along a curved line in north west direction to Zürich 30 km downward. Its width varies between 2.5 and 0.5 km (Fig. 1). At Rapperswil, Lake Zürich is separated by a dam from lake Obersee the outflow of which is the main inflow to Lake Zürich with an average discharge of ~ 76 m^3/s. The only outflow is River Limmat which leaves the lake in Zürich with an average discharge of ~ 90 m^3/s.

Lake Zürich has a surface of 65 km^2, a volume of 3.3 km^3 and an average residence time of ~ 420 days. The deepest location with 137 m depth is close to Thalwil, where one of the six measurement sites of the water quality monitoring program is located (Fig. 1). This paper is based on measurements at this site.

2.2. Data: sources and description

Physical, chemical and biological parameters are monthly measured in the water quality monitoring program by WVZ since 1972 at six locations in the lake. From this large collection of data only data used in this work is described below. A detailed description of the whole data set is available in the form of a technical report (Gammeter et al., 1997).

Chemical and physical parameters: Water temperature and concentrations of oxygen, ammonium, nitrate and phosphate are measured at the site close to Thalwil at depths of 0, 1, 2.5, 5, 7.5, 10, 12.5, 15, 20, 30, 40, 60, 80, 90, 100, 110, 120, 130 and 136 m, respectively. Light attenuation depths to 10, 1 and 0.1% of the surface intensity are also measured by WVZ. An approximation to the light intensity at the lake surface was obtained by using solar radiation data from a measurement site of the Swiss Meteorological Institute (SMA) located in Zürich. Values measured hourly were

converted to monthly averages for use in the model. Averaging sunlight over daily periods implies that a simulation of the diurnal cycle is not in the scope of the model and that light intensities and growth rates used in the model are daily averages that are smaller than instantaneous values during the day. This is an important point to be noted when model parameters are compared with published values.

Biological parameters: Between the water surface and 40 m depth phytoplankton concentrations are measured at the same depth levels as the chemical parameters mentioned above. Below 40 m phytoplankton concentrations are measured at 80, 120 and 136 m depth. From the detailed counting of algal species, in the present work the concentrations of the blue–green algae *Planktothrix (Oscillatoria) rubescens* and the sum of the concentrations of all other algae are used. Zooplankton concentrations are determined in spatially integrated samples between 0 and 20 m ('epilimnion') and 20–136 m ('hypolimnion'). From this data only *Daphnia* concentrations are used. All plankton concentrations were given in units of wet mass (WM). The modelled dry mass (DM) concentrations were multiplied by a factor of five for comparisons with measured wet mass concentrations.

Inflow: Organic particles and the nutrients phosphate, ammonia and nitrate are considered in the inflows from Lake Obersee at Rapperswil, from the sewage treatment plants around the lake and from several small rivers discharging into the lake. In addition, atmospheric deposition of phosphate, ammonia and nitrate is considered. Data from WVZ and reports from the local water protection authority (Amt für Gewässerschutz des Kantons Zürich, AGW) (AGW, 1985) and by the Swiss Federal Institute for Environmental Science and Technology (EAWAG) (EAWAG, 1992) were used to quantify the inflows from Lake Obersee and from small rivers discharging into the lake; data to quantify inflows from sewage treatment plants were obtained from AGW (1992).

3. Review of recent developments in lake water quality modeling

The most important direction of development of lake water quality models in the past decade was towards coupled physical–biological models.

The complexity of the description of the physical processes driving lake stratification and mixing varies considerably among these models. The MINLAKE model (Riley and Stefan, 1988) combines a temperature model by Ford and Stefan (1980) with a relatively simple parameterization of turbulent diffusivity in the epilimnion based on wind velocity and a parameterization based on the Brunt-Väisälä frequency in the hypolimnion. A similar approach is followed in the LIMNMOD model by Karagounis et al. (1993). This model is based on a model for temperature and mixing by Wüest (1987) (see also Wüest et al. (2000)). The DYRESM Water Quality model (Hamilton and Schladow, 1997; Schladow and Hamilton, 1997) is based on an extended version of the DYRESM (Dynamic Reservoir Simulation Model) temperature and mixing model (Imberger and Patterson, 1981). Due to the mechanistic description of physical processes, this mixing and temperature model is free of calibration (Hamilton and Schladow, 1997). The physical submodel of the PROTECH (Phytoplankton RespOnses To Environmental CHange) model (Reynolds and Irish, 1997; Elliott et al., 1999a,b, 2000) is based on the calculation of the epilimnion thickness with the aid of the Monin-Obukhov equation. Details of the physical model equations are not given. In contrast to the previously described one-dimensional lake models CE-QUAL-W2 (Cole and Buchak, 1995) implements two-dimensional hydraulics in a narrow lake, estuary or reservoir. Version 3 of this program, which is currently under development, will even be able to model river basins consisting of river and reservoir segments (Cole and Wells, 2000).

The description of biogeochemical and biological processes varies also significantly among these models. In MINLAKE (Riley and Stefan, 1988), LIMNMOD (Karagounis et al., 1993) and DYRESM Water Quality (Hamilton and Schladow, 1997; Schladow and Hamilton, 1997),

a relatively simple description of phytoplankton by one or only a few functional classes is used in order to describe the key processes affecting nutrient and oxygen concentrations in the lake. All of these models distinguish the steps of nutrient uptake and growth of algae on internally stored nutrients. In contrast to the description of phytoplankton in the models described above, in PROTECH (Reynolds and Irish, 1997; Elliott et al., 1999a,b, 2000) a detailed phytoplankton model with up to eight algal species from a library of 18 species can be used. This model is based on maximum specific growth rates of these species measured under ideal culture conditions. Although the results for individual species do not correspond very well to observations, the results for the sum of all species lead to good agreement with data. This is interpreted as an indication of the need to model one level further down than required for interpretation (Elliott et al., 2000). The water quality component of the two-dimensional model implemented in CE-QUAL-W2 (Cole and Buchak, 1995) can be applied to describe longitudinal concentration variations in narrow reservoirs in addition to vertical variation. However, this model still excludes zooplankton and it contains a simple parameterization of sediment oxygen demand. In Version 3 of this program, which is currently under development, it is planned to include zooplankton as well as a submodel for sediment diagenesis (Cole and Wells, 2000).

The relatively detailed description of processes in the water column in the models described above is in contrast to the effort applied to describe the processes in the sediment. In most models, the effect of mineralisation in the sediment is just described by a given oxygen and nitrate demand and a given ammonia and phosphate release flux out of the sediment. In those models, in which the sediment is taken into account explicitly (Karagounis et al., 1993) a different process formulation is used in the sediment than in the water column. It is a focus of the model used in the present study to combine a relatively simple model for the processes in the water column with a more realistic sediment submodel that explicitly accounts for the mineralisation processes in the sediment based on the same process formulation as in the water column (however, using larger specific mineralisation rates to account for a higher bacterial density).

4. Model description

The model used in this paper is designed to fulfil the following requirements:

- A simple engineering-type model that aggregates algal and zooplankton species as far as possible should be combined with a simple sediment model in which the same process formulations are applied as in the water column.
- A phosphate uptake process on organic particles sinking through the hypolimnion should be considered (Gächter and Mares, 1985; Hupfer et al., 1995).
- A variable stoichiometry of primary production with respect to phosphorus should be used. However, on the time scale of weeks to month relevant for the model, it does not seem to be necessary to distinguish nutrient uptake and growth processes.
- The biogeochemical processes should be presented in a form that is common practice in the description of models for waste water treatment (Henze et al., 1986; Gujer et al., 1995). This notation enhances the readability of the model significantly and it facilitates the development of integrated models at the catchment scale.

The process formulations used for the model were highly influenced by recent developments in river water quality modelling (Shanahan et al., 2001; Reichert et al., 2001; Vanrolleghem et al., 2001); the values of parameters of the plankton submodel by Andersen (1997) and Reynolds (1997).

4.1. Overview

The model is based on horizontally averaged concentrations. This one-dimensional approach is justified if the typical time scale for transformation processes is much larger than the time needed for horizontal mixing. Dissolved and suspended

Table 1
State variables of the lake model

State variable	Unit	Description (concentration of …)
Particulate compounds:		
X_{ALG}	gDM/m^3	Algae without *Planktothrix rubescens* (dry mass without P)
X_{PLR}	gDM/m^3	*Planktothrix rubescens* (dry mass without P)
X_{zoo}	gDM/m^3	Zooplankton (dry mass with Redfield composition)
X_S	gDM/m^3	Biodegradable organic material (dry mass without P)
X_I	gDM/m^3	Inert organic material (dry mass without P)
$X_{P,ALG}$	gP/m^3	Organic phosphorus in algae
$X_{P,PLR}$	gP/m^3	Organic phosphorus in *Planktothrix rubescens*
$X_{P,S}$	gP/m^3	Organic phosphorus in biodegradable organic material
$X_{P,I}$	gP/m^3	Organic phosphorus in inert organic material
$X_{PI,S}$	gP/m^3	Phosphate attached to biodegradable organic material
Dissolved compounds		
S_{HPO4}	gP/m^3	Phosphate-phosphorus
S_{NH4}	gN/m^3	Ammonia-nitrogen
S_{NO3}	gN/m^3	Nitrate-nitrogen
S_{O2}	gO/m^3	Oxygen

substances are transported in the water column by vertical mixing. In addition, algae and suspended particles are transported by sedimentation. Two sediment layers are used to approximately describe substances and processes in the sediment. Suspended particles interact with the sediment layers by sedimentation and diffusive exchange with the sediment pore water affects concentrations of dissolved substances.

In Table 1 all state variables of the model are summarized. The biological part of the model is represented by the three plankton classes *Planktothrix (Oscillatoria) rubescens* (most abundant blue–green algae in Lake Zürich), other algae and zooplankton. The blue–green alga *Planktothrix (Oscillatoria) rubescens* was selected as a separate plankton class because in the average of many years it contributes up to $\sim 20\%$ of the phytoplankton biomass in Lake Zürich (Gammeter et al., 1997), its optimal growth conditions differ significantly from that of other algae and it is of special interest for the water supply authority. Biodegradable and inert organic matter summarize organic particles resulting from allochthonous sources, from death of algae and zooplankton, and from zooplankton excretion as fecal pellets. The phosphorus contents of algae, *Planktothrix (Oscillatoria) rubescens* and organic matter are separate state variables because the variable stoichiometry of primary production leads to a variable phosphorus content of these particles. Zoo plankton, on the other hand, is described with a constant phosphorus content according to the Redfield stoichiometry (Redfield et al., 1966). In addition, the phosphorus content resulting from phosphate uptake by sinking particles is considered as a state variable. According to the explanation of this process given by Hupfer et al. (1995), this state variable is denoted inorganic phosphorus (this point is discussed in more detail in Section 5). Phosphate, ammonium and nitrate are the most relevant nutrients and together with dissolved oxygen represent the dissolved state variables of the model.

4.2. Mass balance equations

In the water column (index: l), the following equation is solved for each dissolved state variable

$$\frac{\partial S_l}{\partial t} = \frac{1}{A}\frac{\partial}{\partial z}\left(AK_z\frac{\partial S_l}{\partial z}\right) + \frac{q}{A}S_{in} - \frac{1}{A}\frac{\partial}{\partial z}(QS_l) + r_l - \frac{1}{A}\frac{dA}{dz}\frac{D\theta}{h_{sed}/2}(S_l - S_{s_1}), \quad (1)$$

and the following equation for each particulate state variable:

$$\frac{\partial X_l}{\partial t} = \frac{1}{A}\frac{\partial}{\partial z}\left(AK_z\frac{\partial X_l}{\partial z}\right) + \frac{q}{A}X_{in} - \frac{1}{A}\frac{\partial}{\partial z}(QX_l) + r_l - \frac{\partial}{\partial z}(v_{sed}X_l). \quad (2)$$

In these equations, S is the concentration of a dissolved compound (ML^{-3}), X is the concentration of a particulate compound (ML^{-3}), t is time

(T), z is the vertical coordinate pointing downwards ($z=0$ at the lake surface) (L), A is the cross-sectional area of the lake (L^2), K_z is the vertical mixing coefficient (L^2T^{-1}), r are transformation rates ($ML^{-3}T^{-1}$), q is the volumetric lateral inflow (rivers and sewage treatment plants are assumed to discharge into the epilimnion) (L^2T^{-1}), S_{in} is the inflow concentration of a dissolved compound (ML^{-3}), X_{in} is the inflow concentration of a particulate compound (ML^{-3}), Q is the volumetric upward flow above lateral inflows (L^3T^{-1}), D is the coefficient of molecular diffusion (L^2T^{-1}), θ is the porosity of the sediment (–), h_{sed} is the thickness of the sediment layers (L), and v_{sed} is the sedimentation velocity (LT^{-1}). In both equations, the first term on the right hand side describes mixing as an effective diffusion process, the second term describes lateral inflow, the third term advection in the water column resulting from lateral inflows (the outflow is at the lake surface) and the fourth term describes the net effect of all transformation processes. The last term of Eq. (1) describes exchange of the dissolved substance with the pore water of the upper sediment layer (index: s_1), the last term of Eq. (2) describes sedimentation of particles through the water column.

Eq. (1) is coupled to the following two equations for dissolved substances in the pore water of the two modelled sediment layers:

$$\frac{\partial S_{s_1}}{\partial t}=\frac{1}{\theta h_{sed}}\left(\frac{D\theta}{h_{sed}/2}(S_l-S_{s_1})+\frac{D\theta}{h_{sed}}(S_{s_2}-S_{s_1})\right)+\frac{r_s}{\theta}. \tag{3}$$

$$\frac{\partial S_{s_2}}{\partial t}=\frac{1}{\theta h_{sed}}+\frac{D\theta}{h_{sed}}(S_{s_1}-S_{s_2})+\frac{r_s}{\theta}. \tag{4}$$

Here, the index s_2 refers to the lower sediment layer. The equation for particulate substances (Eq. (2)) is coupled with the two sediment equations:

$$\frac{\partial X_{s_1}}{\partial t}=\frac{1}{h_{sed}}\left(X_l v_{sed}-\frac{F_{vol,1}}{1-\theta}X_{s_1}\right)+r_s, \tag{5}$$

$$\frac{\partial X_{s_2}}{\partial t}=\frac{1}{h_{sed}}\left(\frac{F_{vol,1}}{1-\theta}X_{s_1}-\frac{F_{vol,2}}{1-\theta}X_{s_2}\right)+r_s \tag{6}$$

where the volumetric particle fluxes between water column and the upper sediment layer, between the two sediment layers and between the bottom sediment layer and the permanent sediment (not modelled) are given as

$$F_{vol,0}=\sum_X \frac{X_l v_{sed}}{\rho}+F_{vol,ext} \tag{7}$$

$$F_{vol,i}=F_{vol,i-1}+h_{sed}\sum_X \frac{r_s}{\rho},\quad i=1,2, \tag{8}$$

where summation is over all particulate substances and $F_{vol,ext}$ is an additional particle flux by substances that are not modelled.

4.3. Physical processes

Vertical mixing: Information about diffusion coefficients was gained from the following sources: Strong mixing in the epilimnion was described with a large effective diffusion coefficient in this zone. The heat budget method (Powell and Jassby, 1974) was used to estimate diffusion coefficients in the metalimnion. Due to the low resolution of temperature data and only small variations between temperature profiles the uncertainty of calculated values was very large. In the hypolimnion for the same reasons the method could not be applied. Additional information about typical diffusion coefficients were taken from Li (1973), where monthly temperature averages over the years from 1948 to 1957 were used for calculation. Phosphate profiles were used as follows, to get information about diffusion in the hypolimnion: During the stagnation period with small exchange between epi- and hypolimnion, the phosphate increase between two profiles was calculated. Assuming a constant phosphate flow and neglecting transformation processes, the heat budget technique was then applied to the phosphate concentration. All this information about diffusion coefficients was then summarized with constant values for summer and winter periods in the epi-, the meta- and the upper and lower hypolimnion. Then time dependent boundaries between these zones were taken from temperature data. A simulation of the temperature with these diffusion coefficients was then performed where the temperature above 10 m depth was given as a boundary condition and small corrections to the

Table 2
Biogeochemical conversion processes with stoichiometric coefficients for all state variables

No.	Process	S_{NH4} $\left[\frac{gN}{m^3}\right]$	S_{NO3} $\left[\frac{gN}{m^3}\right]$	S_{HPO4} $\left[\frac{gP}{m^3}\right]$	S_{O2} $\left[\frac{gO}{m^3}\right]$	X_{ALG} $\left[\frac{gDM}{m^3}\right]$	$X_{P,ALG}$ $\left[\frac{gP}{m^3}\right]$	X_{PLR} $\left[\frac{gDM}{m^3}\right]$	$X_{P,PLR}$ $\left[\frac{gP}{m^3}\right]$	X_{ZOO} $\left[\frac{gDM}{m^3}\right]$	X_S $\left[\frac{gDM}{m^3}\right]$	$X_{P,S}$ $\left[\frac{gP}{m^3}\right]$	$X_{PI,S}$ $\left[\frac{gP}{m^3}\right]$	X_I $\left[\frac{gDM}{m^3}\right]$	$X_{P,I}$ $\left[\frac{gP}{m^3}\right]$
1	Growth ALG		$-a_N$	$-b_P$	1.2	1	b_P								
2	Growth PLR		$-a_N$	$-b_P$	1.2			1	b_P						
3	Growth ZOO	$v_{ZOO,N}$		$v_{ZOO,N}$	$-v_{ZOO,O}$	$-1/Y_{ZOO}$	$-a_{P,ALG}/Y_{ZOO}$			1	f_c/Y_{ZOO}	0			
4	Resp ALG	a_N		$a_{P,ALG}$	-0.94	-1	$-a_{P,ALG}$								
5	Resp PLR	a_N		$a_{P,PLR}$	-0.94			-1	$-a_{P,PLR}$						
6	Resp ZOO	a_N		$a_{P,red}$	-0.94					-1					
7	Death ALG					-1	$-a_{P,ALG}$				$1-f_p$	$(1-f_p)\ a_{P,ALG}$		f_p	$f_p\ a_{P,ALG}$
8	Death PLR							-1	$-a_{P,PLR}$		$1-f_p$	$(1-f_p)\ a_{P,PLR}$		f_p	$f_p\ a_{P,PLR}$
9	Death ZOO									-1	$1-f_p$	$(1-f_p)\ a_{P,red}$		f_p	$f_p\ a_{P,red}$
10	Aer miner	a_N		$a_{P,S}+a_{PI,S}$	-0.94						-1	$-a_{P,S}$	$-a_{PI,S}$		
11	Anox miner	a_N	-0.33	$a_{P,S}+a_{PI,S}$							-1	$-a_{P,S}$	$-a_{PI,S}$		
12	Nitrification	-1	1		-4.6										
13	P−uptake			-1									1		

diffusion coefficients were made in order to get a good agreement between the simulation and the temperature data.

Sedimentation: Particles are assumed to have a constant sedimentation velocity, v_{sed} (LT^{-1}), which is different for different types of particles. The sedimentation velocity of *Planktothrix (Oscillatoria) rubescens*, which regulate their buoyancy with gas vacuoles and of zooplankton, which moves through the lake, was set to zero. The class of other algae was assumed to have a small sedimentation velocity, and the sedimentation velocity of dead organic particles was selected to be relatively large (cf. Table 5)

Gas exchange at the lake surface: Dissolved oxygen exchange is considered as a boundary condition at the lake surface with a flux proportional to the difference of the current oxygen concentration and saturation. The gas exchange velocity, $v_{O2,atm}$ approximated to be constant.

Light absorption: Light intensity is assumed to decrease with water depth. The light extinction coefficient, η (L^{-1}), is assumed to depend linearly on the concentration of suspended particles X_{part} (ML^{-3}):

$$\eta(z) = k_1 + k_2 \cdot X_{part}(z). \quad (9)$$

In this expression, k_1 (L^{-1}) and k_2 ($M^{-1}L^{-2}$) are empirical parameters which were estimated with light and algae data from Lake Zürich, and X_{part} is the sum of all particulate state variables given in Table 1. With these light extinction coefficients, the decrease of light intensity is:

$$I(z) = I_0 \exp\left(- \int_0^z \eta(z) \mathrm{d}z \right), \quad (10)$$

where I_0 denotes the light intensity at the water surface.

4.4. Biogeochemical processes

Table 2 gives an overview of the biogeochemical processes used in the model. Each row in this table represents one process with its stoichiometric coefficients for all state variables involved. Formulas for stoichiometric variables used in this table are given in Table 3. With the process rates given in Table 4, the contribution of a process to the transformation rate of each component is calculated by multiplying the rate with the corresponding stoichiometric coefficient. Nutrient and oxygen dependence is formulated with Monod-type expressions for the transition from unlimited to limited rates. In some cases, multiplication of limiting factors has been shown to give poor results (De Groot, 1983). For this reason, in the case of the dependence of a process rate on more than one nutrient concentration, in accordance with Liebig's law of the minimum, only the most limiting nutrient is considered for reducing the process rate.

The stoichiometric coefficients were calculated with the technique and the spreadsheet provided in Reichert et al. (2001), based on a Redfield composition of all organic particles. Some of the coefficients where then modified to account for the variable stoichiometry of primary production with respect to phosphorus. Because the phosphorus content is very small, the other mass fractions were not corrected in this step.

Table 3
Mathematical expressions for stoichiometric variables used in Table 2

Variable	Algebraic expression
$a_{P,ALG}$	$\frac{X_{P,ALG}}{X_{ALG}}$
$a_{P,PLR}$	$\frac{X_{P,PLR}}{X_{PLR}}$
$a_{P,S}$	$\frac{X_{P,S}}{X_S}$
$a_{PI,S}$	$\frac{X_{PI,S}}{X_S}$
$a_{P,I}$	$\frac{X_{P,I}}{X_I}$
b_P	$\frac{b_{P,min}+b_{P,max}}{2} + \frac{b_{P,max}-b_{P,min}}{2} \cdot \tanh\left(\frac{S_{HPO_4}-S_{HPO_4,crit}}{\Delta S_{HPO_4}}\right)$
Y_{ZOO}	$Y_{ZOO,max} \min\left(1, \frac{a_{P,ALG}}{a_{P,red}}\right)$
F_e	$c_e(1-Y_{ZOO})$
$v_{ZOO,N}$	$a_N \cdot \frac{1-Y_{ZOO}-f_e}{Y_{ZOO}}$
$v_{ZOO,P}$	$\frac{a_{P,ALG}}{Y_{ZOO}} - a_{P,red}$
$v_{ZOO,O}$	$0.93 \cdot \frac{1-Y_{ZOO}-f_e}{Y_{ZOO}}$

Table 4
Process rates of biogeochemical conversion processes

No.	Process	Rate
1	Growth ALG	$k_{\mathrm{gro,ALG},T_0} \cdot \exp(\beta_{\mathrm{ALG}}(T-T_0)) \cdot \frac{I(z)}{K_{\mathrm{I,ALG}}+I(z)} \cdot \min\left(\frac{S_{\mathrm{NO_3}}}{K_{\mathrm{NO_3,ALG}}+S_{\mathrm{NO_3}}}, \frac{S_{\mathrm{HPO_4}}}{K_{\mathrm{HPO_{4,ALG}}}+S_{\mathrm{HPO_4}}}\right) \cdot X_{\mathrm{ALG}}$
2	Growth PLR	$k_{\mathrm{gro,PLR},T_0} \cdot \exp(\beta_{\mathrm{PLR}}(T-T_0)) \cdot \frac{I(z)}{K_{\mathrm{I,PLR}}} \exp\left(1-\frac{I(z)}{K_{\mathrm{I,PLR}}}\right) \cdot \min\left(\frac{S_{\mathrm{NO_3}}}{K_{\mathrm{NO_{3,ALG}}}+S_{\mathrm{NO_3}}}, \frac{S_{\mathrm{HPO_4}}}{K_{\mathrm{HPO_4,ALG}}+S_{\mathrm{HPO_4}}}\right) \cdot X_{\mathrm{PLR}}$
3	Growth ZOO	$k_{\mathrm{gro,ZOO},T_0} \cdot \exp(\beta_{\mathrm{ZOO}}(T-T_0)) \cdot X_{\mathrm{ALG}} \cdot \left(1, \frac{a_{\mathrm{P,ALG}}}{a_{\mathrm{P,red}}}\right) \cdot X_{\mathrm{ZOO}}$
4	Resp ALG	$k_{\mathrm{resp,ALG},T_0} \cdot \exp(\beta_{\mathrm{ALG}}(T-T_0)) \cdot \frac{S_{\mathrm{O_2}}}{K_{\mathrm{O_2resp}}+S_{\mathrm{O_2}}} \cdot X_{\mathrm{ALG}}$
5	Resp PLR	$k_{\mathrm{resp,PLR},T_0} \cdot \exp(\beta_{\mathrm{PLR}}(T-T_0)) \cdot \frac{S_{\mathrm{O_2}}}{K_{\mathrm{O_2resp}}+S_{\mathrm{O_2}}} \cdot X_{\mathrm{PLR}}$
6	Resp ZOO	$k_{\mathrm{gro,ZOO},T_0} \cdot \exp(\beta_{\mathrm{ZOO}}(T-T_0)) \cdot \frac{S_{\mathrm{O_2}}}{K_{\mathrm{O_2resp}}+S_{\mathrm{O_2}}} \cdot X_{\mathrm{ZOO}}$
7	Death ALG	$k_{\mathrm{death,ALG},T_0} \cdot \exp(\beta_{\mathrm{ALG}}(T-T_0)) \cdot X_{\mathrm{ALG}}$
8	Death PLR	$k_{\mathrm{death,PLR},T_0} \cdot \exp(\beta_{\mathrm{PLR}}(T-T_0)) \cdot X_{\mathrm{PLR}}$
9	Death ZOO	$k_{\mathrm{death,ZOO},T_0} \cdot \exp(\beta_{\mathrm{ZOO}}(T-T_0)) \cdot X_{\mathrm{ZOO}}$
10	Aer miner	$k_{\mathrm{miner,aero},T_0} \cdot \exp(\beta_{\mathrm{BAC}}(T-T_0)) \cdot \frac{S_{\mathrm{O_2}}}{K_{\mathrm{O_2,miner}}+S_{\mathrm{O_2}}} \cdot X_{\mathrm{S}}$
11	Anox miner	$k_{\mathrm{miner,anox},\ T_0} \cdot \exp(\beta_{\mathrm{BAC}}(T-T_0)) \cdot \frac{S_{\mathrm{NO_3}}}{K_{\mathrm{NO_3,miner}}+S_{\mathrm{NO_3}}} \cdot \left(1-\frac{S_{\mathrm{O_2}}}{K_{\mathrm{O_2,miner}}+S_{\mathrm{O_2}}}\right) \cdot X_{\mathrm{S}}$
12	Nitrification	$k_{\mathrm{nitri},T_0} \cdot \exp(\beta_{\mathrm{BAC}}(T-T_0)) \cdot \min\left(\frac{S_{\mathrm{O_2}}}{K_{\mathrm{O_2,nitri}}+S_{\mathrm{O_2}}}, \frac{S_{\mathrm{NH_4}}}{K_{\mathrm{NH_4,nitri}}+S_{\mathrm{NH_4}}}\right)$
13	P-uptake	$k_{\mathrm{upt}} \cdot \frac{1}{A}\left\lvert\frac{\mathrm{d}A}{\mathrm{d}z}\right\rvert \cdot \left(a_{\mathrm{P,max}}-\frac{X_{\mathrm{PI,S}}}{X_{\mathrm{S}}}\right) \cdot \frac{S_{\mathrm{O_2}}}{K_{\mathrm{O_2,upt}}+S_{\mathrm{O_2}}} \cdot S_{\mathrm{HPO_4}} \cdot X_{\mathrm{S}}$

All conversion rates depend exponentially on temperature. All processes are active in the water column and in all sediment layers, however, some parameters have different values in the water column than in the sediment (e.g. the light intensity is zero in the sediment and mineralization rates are much smaller in the water column than in the sediment).

The values of the parameters of the biogeochemical processes used for the simulation are listed in Tables 6 and 7.

4.4.1. *Growth processes: algae, Planktothrix rubescens and zooplankton*

Algae: In order to account for the strong phosphorus limitation of algae growth during the summer, algae growth is modelled with a variable stoichiometry with respect to phosphorus. This allows algae to grow with a much smaller phosphorus content if phosphate is present in small concentrations than if it is readily available. In contrast to this consideration of seasonal changes in composition, changes in composition due to different dynamics of nutrient uptake and growth processes (Ketchum, 1939), that could be modelled with the model proposed by Droop (1983), are neglected because they are not relevant on the time scale of operation of the model (months to years).

The stoichiometry of algae growth is described in row 1 of Table 2. It is based on the biomass composition according to Redfield et al. (1966) with the exception of the phosphorus content of the newly built biomass that is assumed to depend on the phosphate concentration in the water. The dependence of the phosphorus content of newly built algae, b_{P}, on phosphate concentration in the

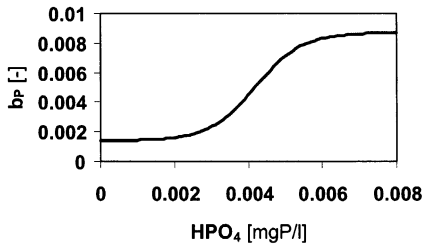

Fig. 2. Dependence of the phosphorus content of newly built algae, b_P, on the phosphate concentration in the water column.

water is formalized by the expression given in Table 3 and shown in Fig. 2. The variability in the stoichiometric coefficient for oxygen caused by the variability in the coefficient of phosphate is neglected. The dependence shown in Fig. 2 leads to algae growth according to the composition proposed by Redfield et al. (1966) if phosphate concentration in the water is high enough, whereas they grow with six times less phosphorus under strongly phosphorus limiting conditions. The necessity of using such a variability in the stoichiometry with respect to phosphorus is known from other lakes (Hupfer et al., 1995). Its necessity for the application of the model to Lake Zürich is discussed in Section 5. Because of the low concentrations of ammonia in the epilimnion and the availability of nitrate, the main nitrogen source for algae growth is assumed to be nitrate. Under different circumstances it may be advantageous to introduce a switching function from ammonia to nitrate, depending on the concentrations of these compounds (Brown and Barnwell, 1987).

The growth rate of algae is given in row 1 of Table 4. Light and nutrient limitations are described with Monod-type rate reduction factors. Only the reduction factor of the most limiting nutrient is considered.

Planktoihrix (Oscillatoria) rubescens: The blue-green algae *Planktothrix (Oscillatoria) rubescens* is a low light specialist that keeps its vertical position with the aid of gas vacuoles at the lower border of the epilimnion (Lampert and Sommer, 1997). In the most parsimonious lake model, *Planktothrix (Oscillatoria) rubescens* could be included in the class summarizing all other algae described above. *Planktothrix (Oscillatoria) rubescens* are considered as an own state variable because they are of special interest for the water supply authority and because their significantly different growth behaviour leads to different growth parameters.

The stoichiometry of growth of *Planktothrix (Oscillatoria) rubescens* given in row 2 of Table 2 is analogous to that of the other algae described above. Also for *Planktothrix (Oscillatoria) rubescens* nitrogen uptake is based on nitrate because of the availability of this nutrient in the epilimnion. An important difference in comparison to other algae in the model is that *Planktothrix* (*Ocillatoria*) *rubescens* are not exposed to grazing by zooplankton (see below).

The growth rate of *Planktothrix (Oscillatoria) rubescens* is given in row 2 of Table 4. It considers light inhibition using the light function proposed by Steele (1962) with a small value for the light intensity at maximum growth, $K_{I,PLR}$. The ability of holding its vertical position is accounted for by setting the sedimentation velocity to zero (see Table 5).

Zooplankton: The simplest possible zooplankton model is used which summarizes all organisms in one class that feeds on algae. In Lake Zürich, *Daphnia* is the most abundant zooplankton species. Because this species has been shown to have a much greater impact on phytoplankton than the other species (Pace, 1984; McQueen et al., 1986), modelled zooplankton concentrations are compared with measurements for *Daphnia*. Investigations of C, N and P content of natural zooplankton populations by Andersen and Hessen (1991) have shown little variations in composition and a constant composition was maintained even in starvation and food enrichment experiments. For this reason, in contrast to algae, zooplankton is modelled with constant elemental mass fractions.

The stoichiometry of growth of zooplankton in the model is given in row 3 of Table 2. The composition of zooplankton is assumed to remain constant at the Redfield values. In order to be able to maintain such a fixed composition under varying phosphorus content of the food ($a_{P,ALG}$)

the yield (Y_{ZOO}) must decrease with decreasing phosphorus content of the food. This means that more algal biomass is consumed to build one unit of zooplankton biomass if the phosphorus content of the algae is low. Many studies support this idea of nutrient limited zooplankton growth (Elser and Hassett, 1994; Sommer, 1991; Urabe and Watanabe, 1992; Hessen, 1992). This phosphorus limitation is modelled with a yield that is proportional to the phosphorus content if the phosphorus content is below the Redfield value (Table 3). The variable f_e describes the fraction of consumed organic matter that is excreted as fecal pellets (the fraction Y_{ZOO} is converted to zooplankton biomass, the fraction $1-Y_{ZOO}-f_e$ is mineralized). Because the yield depends strongly on the phosphorus content of the food, f_e is parameterized with the parameter c_e which specifies the fraction of organic matter not used for zooplankton biomass that is excreted as fecal pellets (the fraction $1-c_e$ is mineralized). c_e rather than f_e is assumed to be independent of the phosphorus content of the food. It is assumed that all phosphorus that is not incorporated into zooplankton biomass is released in the form of phosphate so that the phosphorus content of fecal pellets is zero. This is a rather crude approximation to the low observed phosphorus content of fecal pellets (H.R. Bürgi, personal communication) which had probably to be changed for a less phosphorus limited lake.

The growth rate of zooplankton is given in row 3 of Table 4. It is proportional to the product of food and zooplankton concentrations. A limiting factor proportional to the phosphorus content of the food leads to a reduction of the growth rate if the phosphorus content is below the Redfield value. Note that for the grazing rate of algae this factor is compensated by the same factor in the yield (Tables 2 and 3). This means that the grazing rate of algae is independent of their phosphorus content.

4.4.2. Algae and zooplankton respiration

The processes of algae and zooplankton respiration describe maintenance of these organisms at the expense of their own biomass. These processes are difficult to identify because (usually) only net growth is observed (identifiability becomes even worse with the introduction of death processes below). Nevertheless the process is introduced because spatial separation of growth and respiration can be important in lakes. In the epilimnion, respiration just leads to a reduction in observed growth rates. However, if algae sink and respire in the metaliminon, where light conditions do not allow them to grow, respiration can contribute to the observed metalimnic oxygen minimum.

The stoichiometry of algae, *Planktothrix (Oscillatoria) rubescens* and zooplankton respiration are described in rows 4–6 of Table 2. The three processes are similar with the minor difference, that phosphate release by respiring algae and *Planktothrix (Oscillatoria) rubescens* depends on their current phosphorus content, a_{ALG} and a_{PLR}, respectively, whereas phosphate release by respiring zooplankton is constant because of the constant elemental composition of zooplankton.

The process rates of algae, *Planktothrix (Oscillatoria) rubescens* and zooplankton respiration are given in the rows 4–6 of Table 4. The rates are proportional to the concentration of the respired species with limiting factors with respect to oxygen and with the same temperature dependence as the corresponding growth processes.

4.4.3. Death processes

Death processes transform algae, *Planktothrix (Oscillatoria) rubescens* and zooplankton into degradable and inert organic material. Although it is not relevant if an algae sinking to the sediment is dead or alive (this means that it would again start primary production if exposed to light), the death processes simplify the model because they cause the sediment to consist (nearly) only of the model compounds of degradable and inert organic matter.

The stoichiometry of the death processes is given in rows 7–9 of Table 2. Algae, *Planktothrix (Oscillatoria) rubescens* and zooplankton are converted to a fraction 1-f_p of degradable organic material and a fraction f_p of inert organic material.

The process rates of the death processes are given in the rows 7–9 of Table 4. They are proportional to the current concentration and

have the same temperature dependence as the growth processes.

4.4.4. Mineralization processes

Mineralization processes account for bacterially mediated oxidation of degradable organic matter. Since bacteria are not modelled as state variables, a constant maximum mineralization rate is assumed and only limitation terms for degradable organic matter and oxidants are considered. Only aerobic mineralization using dissolved oxygen and anoxic mineralization using nitrate as the oxidant (denitrification) are used in the model. These two processes are known to be very important for the lake. The first process leads to a significant reduction of oxygen concentrations in the deep hypolimnion, the second to a large nitrogen elimination in the lake (Mengis et al., 1997). It is assumed that the turnover rates of all other oxidation processes (taking place in deeper sediment layers) are small compared to the turnover rates of these two oxidation processes. While this assumption seems reasonable for Lake Zürich, in highly eutrophic lakes with very small oxygen concentration in the deep water anaerobic mineralization processes can become relevant.

The stoichiometries of aerobic and anoxic mineralization are given in the rows 10–11 of Table 2. The nitrogen balance is not closed for anoxic mineralization because molecular nitrogen gas (N_2) escaping from the lake is not considered as a state variable in the model. Because the desorption rate of phosphate adsorbed to organic particles is not significantly different from the mineralization rate in the sediment (Hupfer et al., 1995), desorption of adsorbed phosphate was included in the stoichiometry of the mineralization process (see below for a discussion of phosphate adsorption on organic particles).

The process rate of aerobic mineralization given in row 10 of Table 4 has a Monod-type limitation factor with respect to oxygen. The rate of anoxic mineralization given in row 11 of Table 4 has an inhibition factor with respect to oxygen and a limitation factor with respect to nitrate. Because oxygen concentrations in Lake Zürich are never very low, significant anoxic mineralization (denitrification) only occurs in the sediment. The rate parameters $k_{\mathrm{miner,aero},T_0}$ and $k_{\mathrm{miner,anox},T_0}$ are much higher in the sediment than in the water column in order to account for the much higher bacterial density in the sediment.

4.4.5. Nitrification

The stoichiometry of nitrification is given in row 12 of Table 2. Ammonia is oxydized to nitrate with consumption of oxygen.

The process rate of nitrification is given in row 12 of Table 4. There are limitation factors for ammonia and oxygen. Similarly to mineralization discussed above, the maximum rate, k_{nitri,T_0}, is larger in the sediment than in the water column to account for the higher bacterial density.

4.4.6. Uptake and release of phosphate

In many lakes, it can be observed that phosphate concentrations are very low during the summer not only within the photic zone, where it is consumed by growing algae, but also below. This can be explained with a phosphate uptake process on sinking particles. The existence of such a process has been confirmed by investigating organic particles from sediment traps at different water depths in Lake Sempach (Gächter and Mares, 1985; Hupfer et al., 1995). It was shown that particles became enriched with inorganic phosphorus while settling through the hypolimnion, whereas the organic phosphorus content did not change significantly. One hypothesis for an explanation of this observation is that manganese and iron oxidising bacteria of the type *Metallogenium* form iron hydroxyde surfaces on which inorganic phosphorus adsorbs abiotically (Gächter and Mares, 1985). However, there may be other processes contributing to the observed increase in inorganic phosphorus content of the sinking particles. In order to account for this observation a process of phosphate uptake by organic particles was included in the model and the corresponding phosphorus was denoted 'inorganic phosphorus'. Note, however, that the chosen macroscopic model formulation does not depend on the microscopic mechanism of this uptake process which needs to be further investigated.

The stoichiometry of this phosphate uptake processes is very simple. It is given in row 13 of

Table 2. As mentioned above, desorption is included in the mineralization process given in rows 10–11 of Table 2.

The transformation rate of the phosphorus uptake process is given in row 13 of Table 4. It constitutes an empirical parameterization of the poorly understood process, that is able to account for its macroscopic effects. The formulation of a more universal transformation rate needs more investigations on the microscopic mechanisms leading to phosphate uptake. Because iron diffusing out of the sediment could be the source for the build up of iron oxide surfaces to which phosphate adsorbs, the uptake rate is assumed to be proportional to the sediment area per unit of lake volume, $1/A \cdot \mathrm{d}A/\mathrm{d}z$. In fact, the iron profiles at the deepest point of the lake close to Thalwil show such an increase in iron concentrations in the deepest part of the lake due to an iron release from the sediment. In these profiles there is, however, no indication for such a release in the upper parts of the lake. Fig. 3 shows a comparison of time series of iron concentrations in 24 m depth at Stäfa (close to the sediment) and in 30 m at Thalwil (lake depth at Thalwil 137 m). This comparison shows that iron concentrations in Stäfa, where the measurement is close to the sediment, are often significantly higher than in Thalwil. Due to horizontal mixing, this horizontal inhomogenity is probably smoothed out very rapidly. Nevertheless, it demonstrates that the process of phosphate adsorption to iron hydroxide surfaces could also be of importance in the upper hypolimnion. The uptake rate contains a limiting term with respect to oxygen to account for the oxidation of the iron diffusing out of the sediment to iron hydroxide surfaces at which phosphate adsorbs.

4.5. Model implementation

The model was implemented using the simulation and data analysis software for aquatic systems, AQUASIM (Reichert, 1994, 1998), version 2.1β (see http://www.aquasim.eawag.ch for topical details on this program). Within a spatial configuration consisting of compartments and links of the available types, this program allows its users to define any state variables and transformation processes and to perform simulations, parameter estimations and sensitivity analyses. In order to solve the partial differential Equations 1–8 numerically, in a first step this program discretizes the space derivatives. In a second step, the spatially discretized partial differential equations are integrated in time with the implementation DASSL (Petzold, 1983) of the implicit (backward differencing) variable-step, variable-order GEAR integration technique (Gear, 1971). For the minimization of the sum of weighted squares of the deviations between model results and measurements required for parameter estimation, two numerical techniques were used. The simplex method of Nelder and Mead (1965) was used to find a direction of decrease of the sum of squares far away from the minimum and for parameter estimations with a large number of parameters, whereas the secant method of Ralston and Jennrich (1978) was used for final convergence of identifiable parameter sets. For both techniques the constrained minimization algorithms implemented in AQUASIM were used.

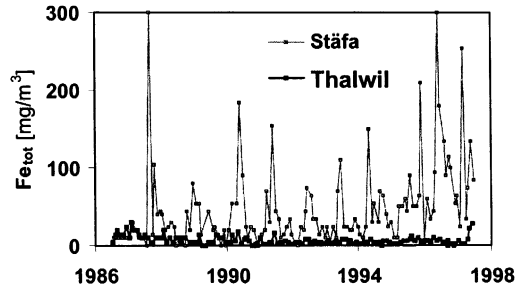

Fig. 3. Time series of total iron concentration in 24 m depth at Stäfa (lake bottom at 25 m) and in 30 m depth at Thalwil (lake bottom at 137 m) show a horizontal inhomogeneity with increased iron concentrations in Stäfa. This is probably caused by iron diffusing out of the sediment.

5. Results and discussion

Compared to the complexity of the real system, the biogeochemical model presented in section 4 (Tables 2–4) is relatively simple. However, from the point of view of parameter identification, the model is rather complex. Obviously, it is not

possible to determine the values of all model parameters with the monthly measured profiles of oxygen, nitrate, ammonia, phosphate, *Planktothrix (Oscillatoria) rubescens*, other algae and zooplankton.

For this reason, we started with literature values for all parameters and iteratively changed the values of those parameters that were assumed to be inaccurately known and had a significant influence on the model results. When the simulations led to qualitative agreement with the measurements, we started a formal sensitivity, identifiability and uncertainty analysis of the model based on the given layout of the measurement. This analysis is only briefly summarized here; a detailed description is given elsewhere (Omlin et al., 2001). The analysis was based on work by Brun et al. (2001) and consisted of the following steps:

Based on prior knowledge and on the expected identifiability, model parameters were grouped into parameters potentially to be estimated from the data and parameters to be determined from other sources. Typically, kinetic parameters specific for the populations in Lake Zürich were potentially to be estimated, stoichiometric, physical and input parameters were assumed to be known from other sources (this distinction had to be made, because it is not possible to estimate input parameters, kinetic and stoichiometric parameters at the same time with the available data). Because the sharp spatial location of the *Planktothrix (Oscillatoria) rubescens* peaks, which often consisted of only one or two data points, kinetic *Planktothrix (Oscillatoria) rubescens* parameters were also excluded from the formal parameter estimation procedure, but they were adapted empirically.

Based on prior estimates of parameter uncertainty and on linear error propagation of this uncertainty through the model, a sensitivity ranking of the model parameters according to their contribution to prediction uncertainty was made.

Based on this sensitivity ranking and on information on potential identifiability problems gained by an analysis of approximate linear dependence of sensitivity functions (Belsley et al., 1980; Belsley, 1991; Brun et al., 2001), parameter sets were selected for weighted least squares parameter fits based on data for the years 1988 and 1989.

The results were analysed for the quality of fit and for reasonableness of estimated parameter values and all the steps were iteratively repeated until convergence occurred (both sensitivity ranking and approximate linear dependence analysis of sensitivity functions are local analyses that depend on the selected parameter values).

This procedure finally led to the simulations and parameter sets shown and discussed in this paper. This seems to be a reasonable parameter set (comparing parameter values with the literature) and it leads to a relatively good approximation of the results with measurements (cf. Sections 5.1–5.2). However, this parameter set is not unique. More experimental investigations and comparisons with data from other lakes are necessary in order to find a more universal and unique parameter set.

In Section 5.1, calculations based on these parameter values are compared with measurements (Figs. 4–9) in order to demonstrate the degree of agreement and to discuss the most important phenomena visible in the data. In Section 5.2, sedimentation fluxes of organic particles and of particulate phosphorus are compared with data from an earlier measurement period (because no data on particle fluxes was available for the simulation period). In Section 5.3, calculated conversion rates of oxygen, nitrate and phosphate are discussed. Finally, in Section 5.4, by a comparison with simplified models, the necessity of using a variable stoichiometry of primary production and of including a phosphate uptake process on sinking particles in the model is justified.

5.1. Concentration profiles

In this section, an overview is given of the results of the simulations for the years 1989 and 1990. These simulations were performed with the parameter values given in Tables 5–7. As described above, 1989 is the second year of the parameter fit and 1990 is the first year of extrapolation. For the year 1990, this is an extrapolation with respect to the biogeochemical part of the model only. Input, light intensity and vertical

mixing parameters of the lake were determined as described in Sections 2.2 and 4.3 with measured data from the corresponding years.

5.1.1. Oxygen and nutrients in the water column

Measured and simulated oxygen and nutrient profiles in the lake are compared in Figs. 4–6.

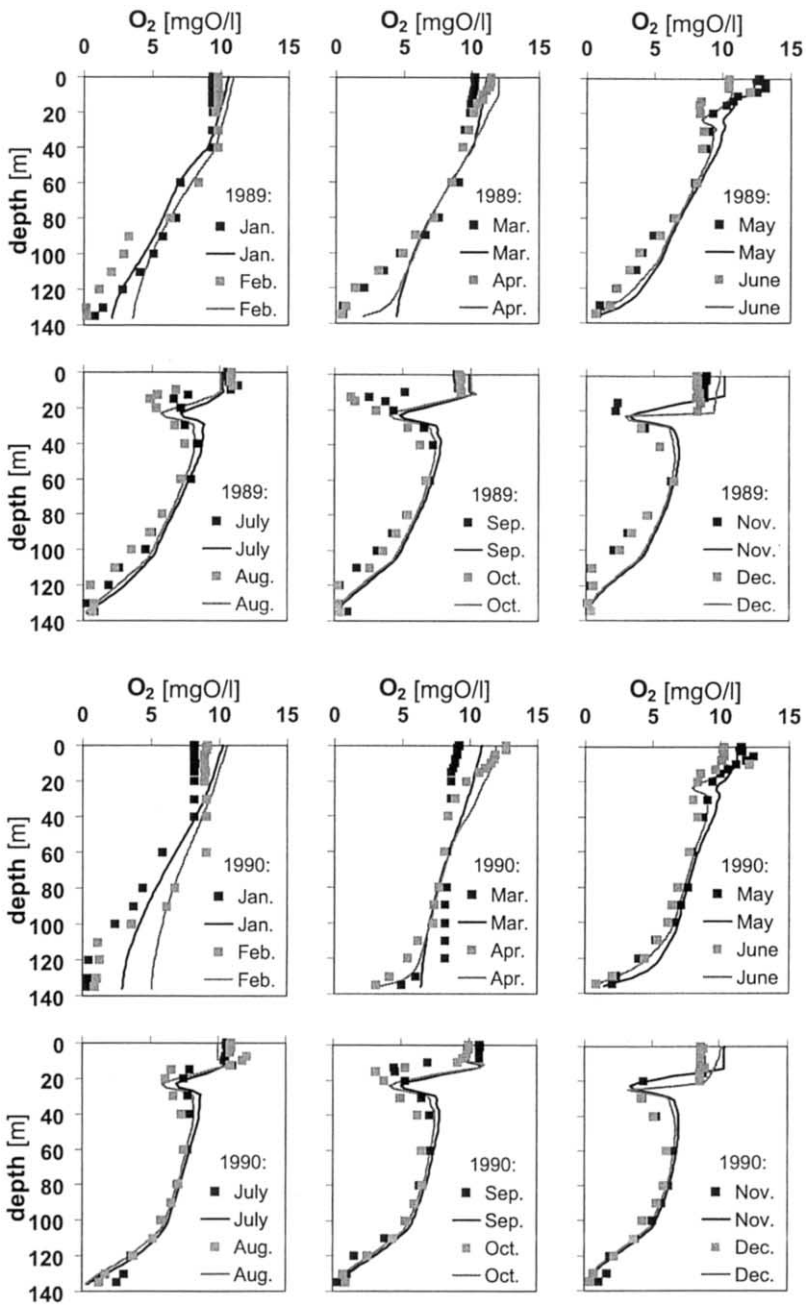

Fig. 4. Simulation and data of monthly oxygen profiles in 1989 (second year of the fit, top) and 1990 (first year of extrapolation, bottom). Markers represent measurements, lines simulated concentrations.

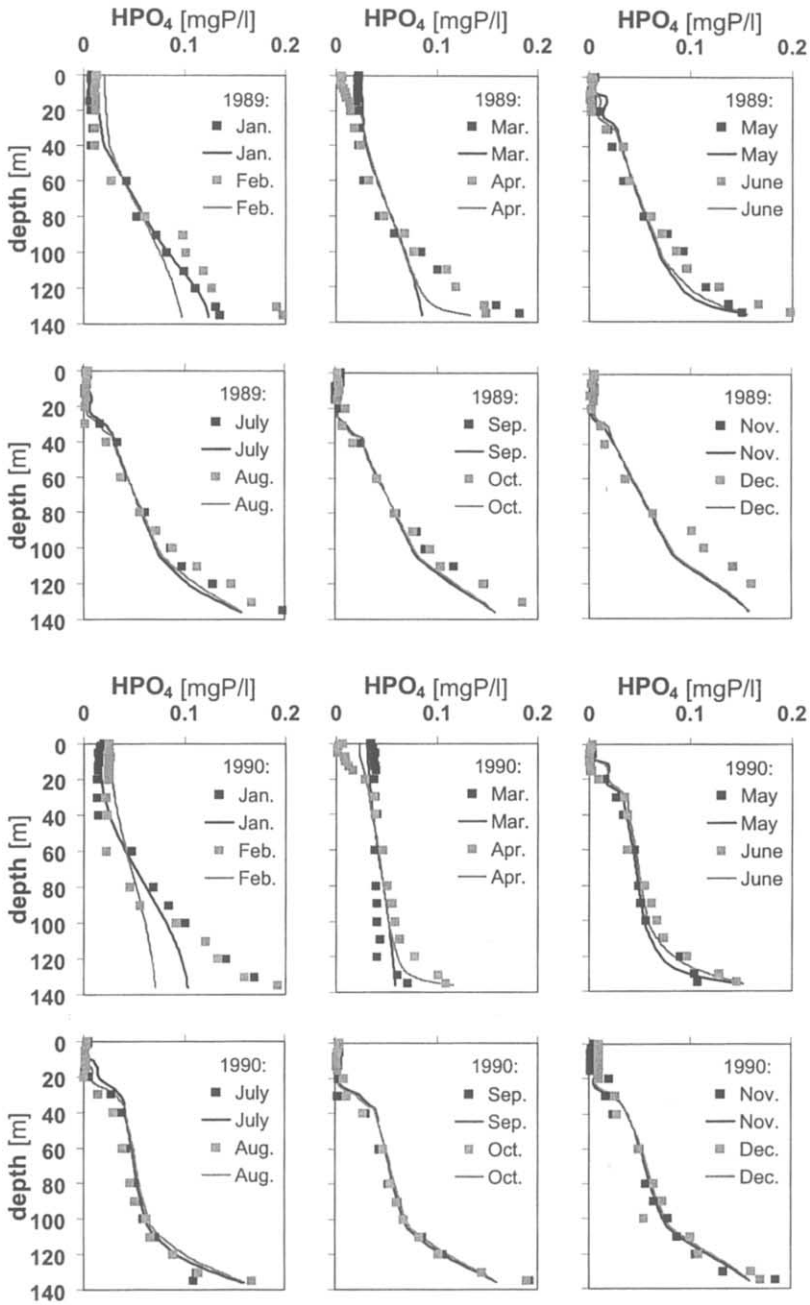

Fig. 5. Simulation and data of monthly phosphate profiles in 1989 (second year of the fit, top) and 1990 (first year of extrapolation, bottom). Markers represent measurements, lines simulated concentrations.

The oxygen data points in Fig. 4 show a strong decrease in oxygen concentration in the metalimnion and close to the lake bottom while in the epilimnion oxygen concentrations remain high. These effects are reproduced at least qualitatively by the simulation. Systematic deviations of the calculation from the measurements in the year 1989 and in the first few months of the year 1990

seem to be mainly caused by inaccuracies in the description of mixing processes during the winter (also in 1989 the oxygen is mixed down into the deep hypolimnion during the first few months of the year). The metalimnic oxygen minimum in the simulation is caused by respiration of sinking algae and by mineralization of organic particles in the sediment at this depth. As diffusive vertical

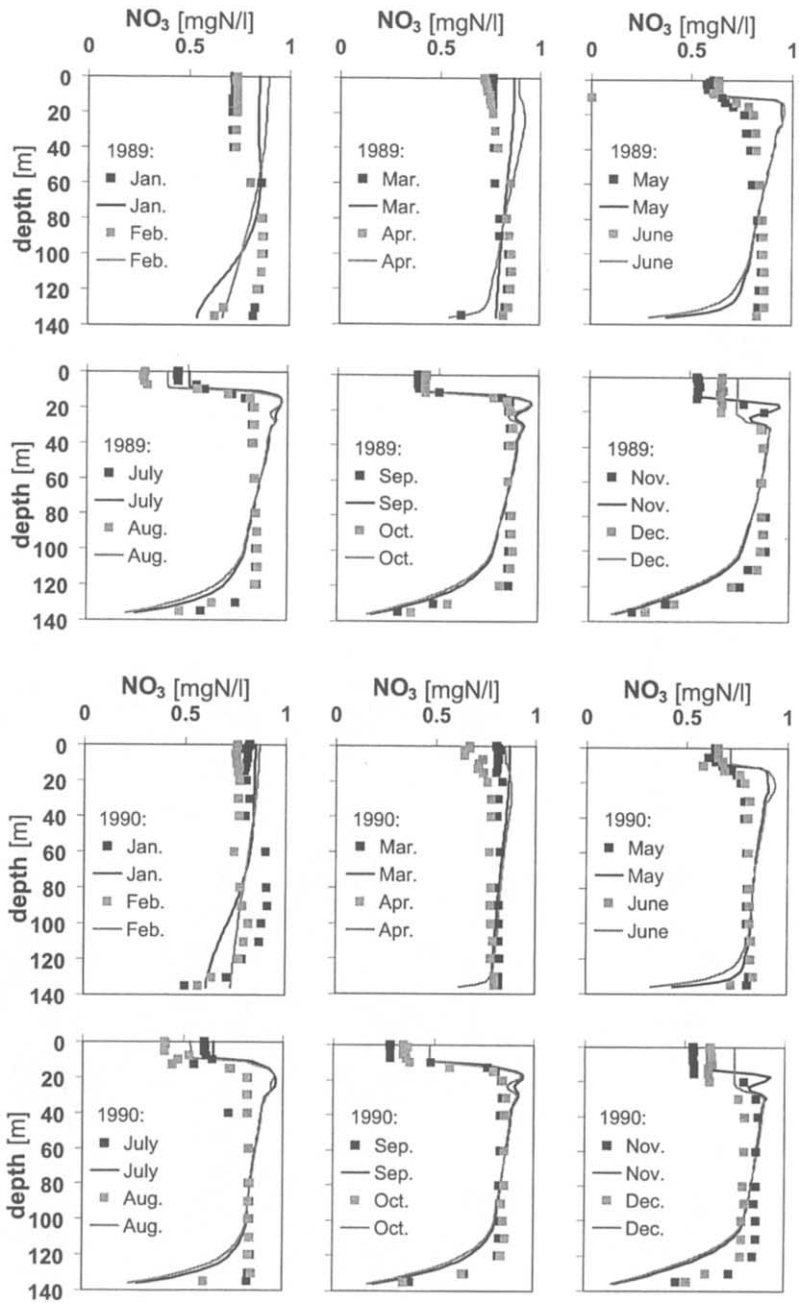

Fig. 6. Simulation and data of monthly nitrate profiles in 1989 (second year of the fit, top) and 1990 (first year of extrapolation, bottom). Markers represent measurements, lines simulated concentrations.

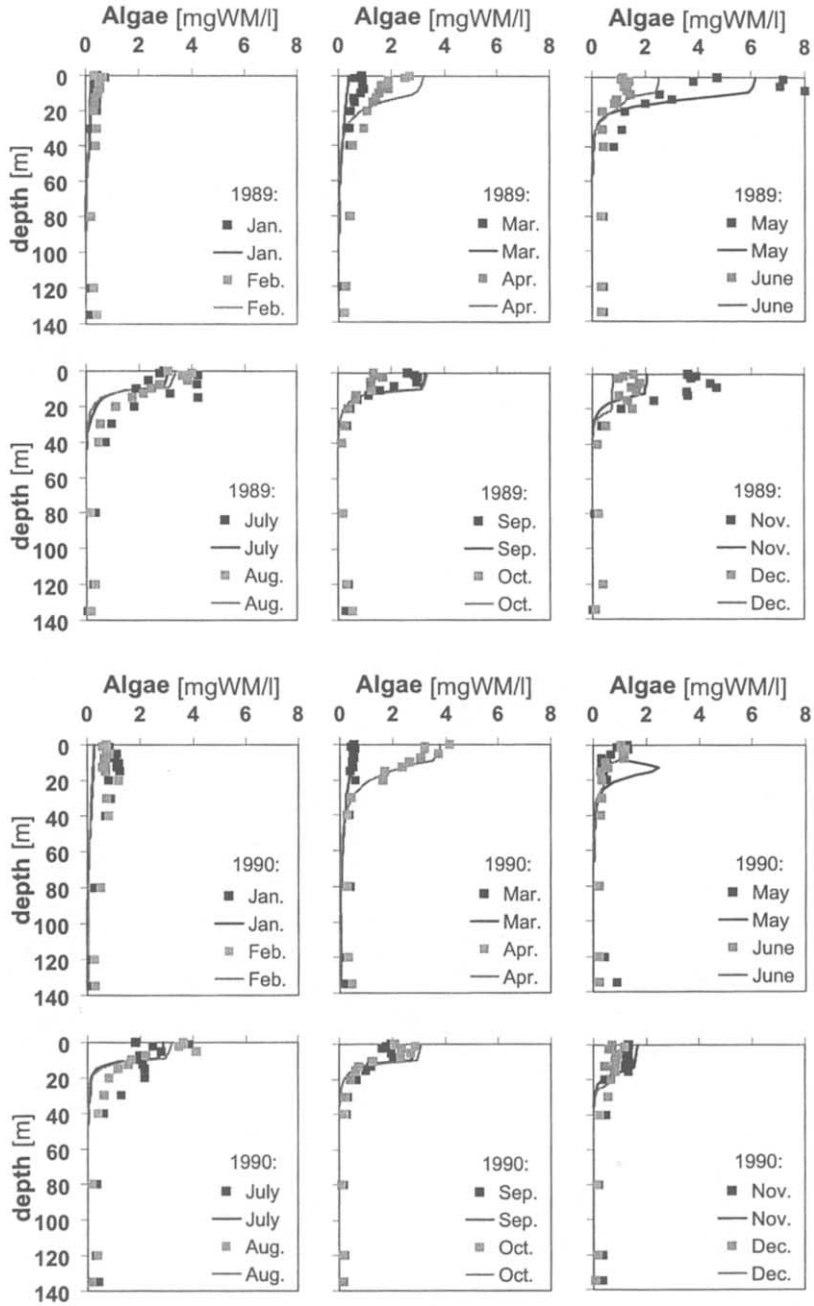

Fig. 7. Simulation and data of monthly algae profiles in 1989 (second year of the fit, top) and 1990 (first year of extrapolation, bottom). Markers represent measurements, lines simulated concentrations.

mixing is very small in the metalimnion, these processes lead to a significant decrease in oxygen concentration. Due to the large sediment surface at this depth, mineralization in the sediment is the dominant cause of this oxygen depletion in the simulation.

The measured phosphate profiles show clearly the phosphate limitation of algal growth during the summer (concentrations in the epilimnion are almost zero) and the significant upward flux of phosphate released by mineralization in the sediment (increasing concentrations in the depth of the lake, especially in the second half of the year). During the summer, phosphate concentra-

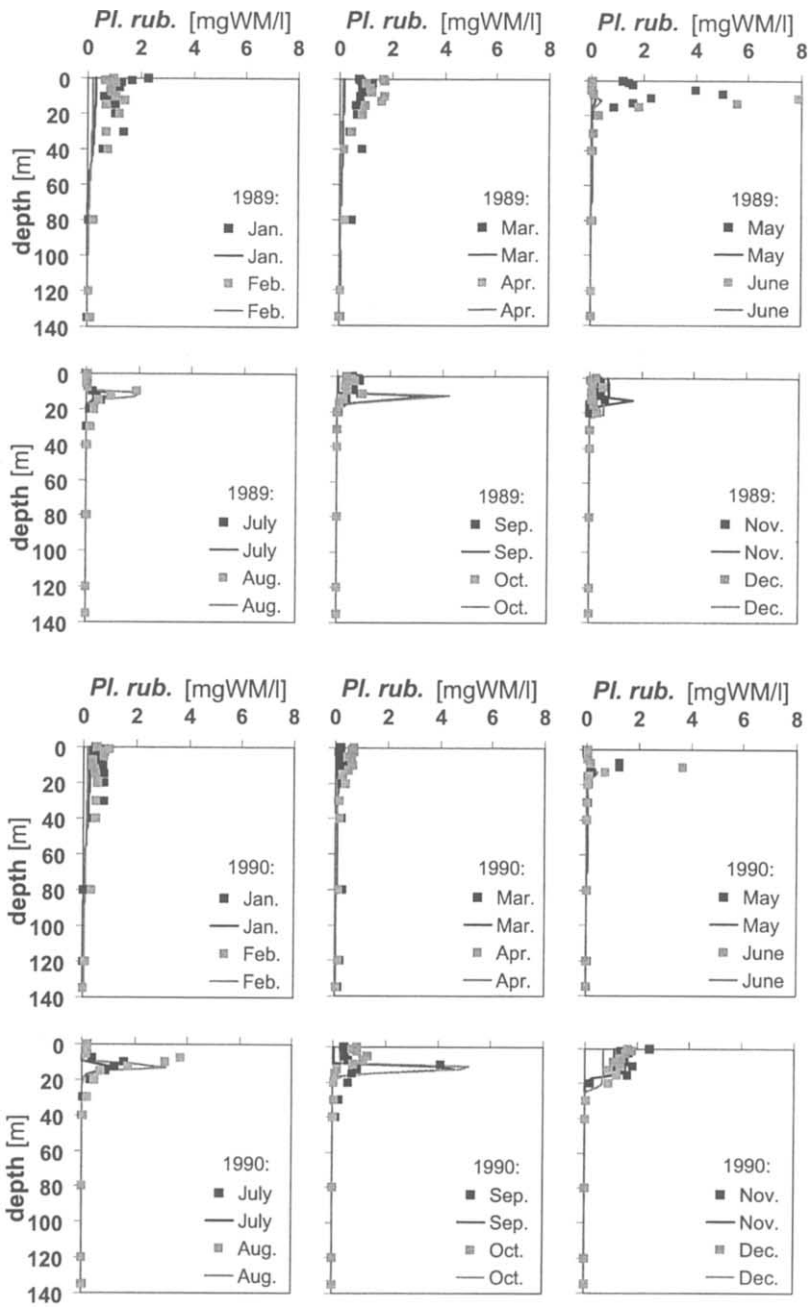

Fig. 8. Simulation and data of monthly *Planktothrix (Oscillatoria) rubescens* profiles in 1989 (second year of the fit, top) and 1990 (first year of extrapolation, bottom). Markers represent measurements, lines simulated concentrations.

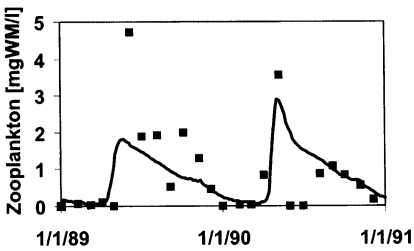

Fig. 9. Simulation and data of zooplankton concentration in the epilimnion over the simulation period 1989-1990. Markers represent measurements for *Daphnia*, the line represents simulated concentrations.

tions are not only very low in the epilimnion, where phosphate is consumed by primary production, but also below in the metalimnion. This is an indication for the significance of a phosphate uptake process on sinking particles (cf. Section 5.4 below). Simulated phosphate profiles represent all these effects and agree very well with measurements in both years (Fig. 5). Again, the deviations between calculation and measurements in the first few months of both years indicate an overestimation of mixing in the deep hypolimnion during the winter.

The significant decrease of nitrate concentrations in the epilimnion during the summer is caused by incorporation of nitrogen into algal biomass and subsequent export by sedimentation. This phenomenon is qualitatively reproduced by the model (cf. Section 5.4 below). However, there is a systematic deviation of the shape of the calculated nitrate profile from the measurements. The significant amount of denitrification in the sediment (cf. Section 5.3) causes the calculated nitrate concentrations to decrease with increasing distance from the water surface. This phenomenon does not occur in the data, with exception of the deepest hypolimnion. The measured constant nitrate concentrations between 20 and 120 m depth could only be reproduced with a significantly higher effective diffusion coefficient in this range of depth of the lake. Such an enlarged diffusion coefficient, however, would destroy the oxygen and phosphate profiles shown in Figs. 4 and 5.

5.1.2. Algae and zooplankton

Measured and simulated profiles of algae and of *Planktothrix (Oscillatoria) rubescens* are compared in the Figs. 7 and 8. Fig. 9 shows a comparison of measured and simulated time series of zooplankton averaged over the epilimnion.

In early spring the stratification of the water column enables net growth of algae (Fig. 7) in the photic layer of the lake. After reaching a maximum in May 1989 and April 1990, respectively, the algae concentration is reduced drastically by grazing of zooplankton and recovers then during the following months. The simulation agrees very well with measurements, what is especially remarkable for the extrapolation in 1990.

Planktothrix (Oscillatoria) rubescens reaches its maximum growth rate at light intensities typical for the metalimnion and is usually light inhibited in the epilimnion. This leads to the sharp peaks visible in the measurements as well as in the simulation (Fig. 8). However, the seasonal variation of *Planktothrix (Oscillatoria) rubescens* is poorly described by the model. Whereas the simulations are in agreement with the measurements during the second half of both years, the observed high concentrations of *Planktothrix (Oscillatoria) rubescens* in May and June are not reproduced by the model.

The dynamics of the zooplankton population strongly depends on the algae concentration. The algae maximum in spring is followed by a maximum of zooplankton concentration (Fig. 9) that leads to a significant decrease in algae concentration. The order of magnitude of the zooplankton concentrations as well as the point in time of the first maximum is very well reproduced by the model. However, after the first maximum, measurements show a stronger variation with a significant decrease followed by a second peak. This dynamics is not reproduced by the simple zooplankton submodel selected for our model. A more detailed zooplankton submodel that distinguishes different classes of species and takes into account grazing of zooplankton by other species of zooplankton is probably necessary to describe the observations in more detail. Such a model should probably also consider more classes of algae and would therefore increase model complexity considerably.

5.2. Sedimentation fluxes

Fig. 10 shows a comparison of sedimentation fluxes for particulate organic carbon and for particulate phosphorus calculated for 1990 and measured by Sigg et al. (1987) in 1984 (there are no data available for other years). These data have not directly been used for model calibration, however, the ratio of the fluxes for organic carbon and for phosphorus has been used for the selection of the value of the parameter $a_{P,max}$. The comparison shows that the qualitative behaviour of these fluxes is represented correctly by the model. Especially, the interannual variation is represented very well. The fluxes seem to be somewhat larger in the simulation for 1990 than measured in 1984. However, the difference is not larger than intraannual differences can be expected to be.

5.3. Oxygen, nitrate and phosphate conversion rates

Fig. 11 shows calculated conversion rates of oxygen, nitrate and phosphate in September 1989 in the water column and in the upper sediment layer (the conversion rates in the lower sediment layer were much smaller). For better comparability, the conversion rates in the sediment layer have been converted to water column-equivalent rates by multiplying them with $h_{sed}/A \cdot |dA/dz|$.

The conversion rates of oxygen in the water column show a maximum of production in the epilimion (significantly larger than the scale of the diagram) and a smaller maximum in ~ 12 m depth in the metalimnion. This lower maximum is caused by the growth of *Planktothrix (Oscillatoria) rubescens*, whereas the upper maximum is caused by the growth of the other algae. Everywhere else, oxygen production is negative due to respiration, grazing, mineralization and nitrification. The sediment layer leads to a higher contribution to oxygen consumption than the water column (mainly due to mineralization).

The nitrate conversion rates show an intensive nitrate consumption due to primary production in the epilimnion and a smaller consumption due to *Planktothrix (Oscillatoria) rubescens* growth in a depth of ~ 12 m. In the rest of the water column, nitrate is produced by nitrification of ammonia diffusing out of the sediment, where it is produced by aerobic and anoxic mineralization. In a more detailed model with a more accurate resolution of the sediment, part of the nitrification shown here in the water column (because there is not enough oxygen in the upper sediment layer) could also occur in the highest mm of the sediment. In the sediment layer, nitrate is denitrified by anoxic mineralization.

Finally, phosphate is consumed in the water column by primary production in the epilimnion and by phosphate uptake in the hypolimnion. It is produced in the sediment layer by aerobic and anoxic mineralization.

5.4. Variable stoichiometry and phosphate uptake

Fig. 12 shows a comparison of measured concentration profiles of nitrate and phosphate during a typical summer situation (September 1989) with simulations for the model described in this paper, for a simplified model without phosphorus uptake on sinking particles, and for an even simpler model without phosphorus uptake and with a constant (Redfield) stoichiometry of algal growth. The equations of the simplified models were the same as those of the full model with exception of the changes mentioned above and the values of the maximum specific growth rates of algae and zooplankton and the sediment layer thickness for which a new fit has been done to allow for an optimal correspondence with the measurements.

Omission of the phosphate uptake process does only insignificantly change the nitrate profiles (the changes are mainly due to the changes in model parameters during the fit). However, the phosphate profiles calculated with this model show two significant deficits: First, the thickness of the surface layer within which phosphate concentrations become very low is significantly too small and second, the gradient of the phosphate profile in the hypolimnion is too small as well. The first observation is a result of the fact that phosphate is only incorporated into algal

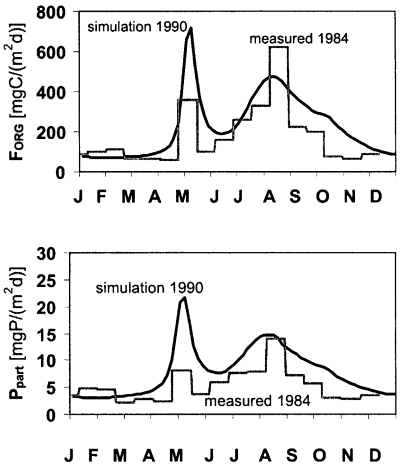

Fig. 10. Calculated particulate organic carbon flux (top) and particulate phosphorus flux (bottom) in 130 m depth. Comparison of the simulation for 1990 with measurements by Sigg et al. (1987) from 1984.

biomass within the photic zone of the lake and that there is no other significant process that consumes phosphate below if the uptake process is turned off. The second observation indicates a too small upward flux of phosphate released from the sediment. The introduction of the phosphate uptake process on sinking particles solves both problems: First, the uptake process decreases the concentrations below the epilimnion, and second, due to the increased downward flux of phosphate attached to sinking particles, a higher phosphate release from the sediment is possible (in the model the attached phosphate is released at the same specific rate as the organic material is mineralized).

The phosphate profiles of the model that, in addition to the omission of the phosphorus uptake process, keeps the phosphorus content of growing algae constant are only insignificantly different from the results of the model that only turns off the uptake process. However, due to the higher phosphorus content of growing algae, much less algal biomass can be produced during this phosphorus limited period. This leads to a significantly smaller reduction of nitrate concentration in the epilimnion. In the model with a variable stoichiometry that decreases the phosphorus content of newly built algae during phosphorus limited periods, much more biomass can be produced under phosphorus limiting conditions. This leads to the observed higher nitrate uptake in the epilimnion. A variability of the phosphorus content of algae as implemented in the model is confirmed by more direct measurements of the composition of algae in other lakes (Hupfer et al., 1995).

6. Conclusions

A biogeochemical lake model was presented and applied to data from Lake Zürich, Switzerland. The one-dimensional model resolves the depth of the lake and calculates nutrient, oxygen and plankton dynamics averaged over daily fluctuations. The model considers growth, respiration and death of two classes of algae and one class of

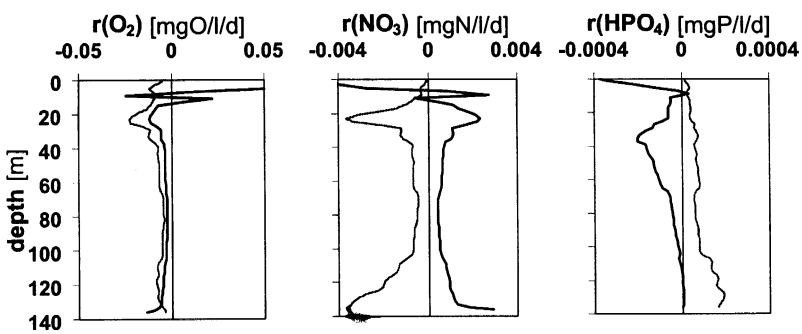

Fig. 11. Oxygen (left), nitrate (middle) and phosphate (right) conversion rates in September 1989 in the water column (black) and in the sediment (converted to water column-equivalent rates, grey).

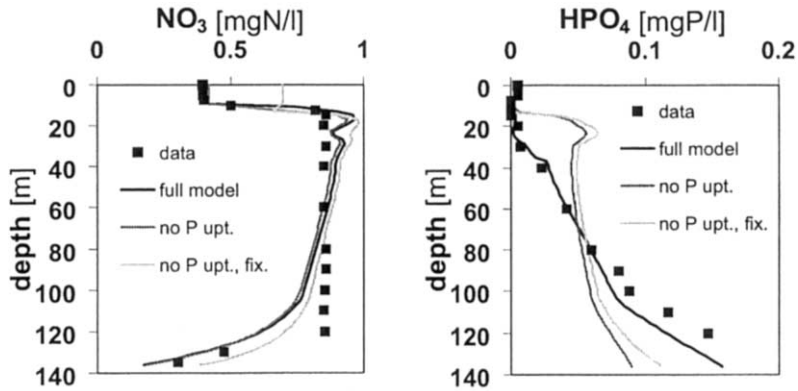

Fig. 12. Comparison of the resulting phosphate and nitrate profiles in September 1989 for the full model described in this paper (black lines), for a model with omission of the phosphate uptake process on sinking particles (dark grey lines) and for a model with omission of the phosphate uptake process and with a constant (Redfield) stoichiometry of algal growth (light grey lines).

zooplankton, mineralization, nitrification, mixing, sedimentation and phosphate uptake on sinking particles. Due to the consideration of a roughly discretized sediment layer, it is able to describe the accumulation of organic matter in the sediment and the subsequent release of nutrients originating from mineralization.

After the calibration of mainly kinetic model parameters (cf. Omlin et al. (2001) for more details of the applied calibration, identifiability and uncertainty analysis procedures), the model was able to reproduce the essential properties of the nutrient, oxygen and plankton dynamics in the lake over several years (cf. Section 5.1). Also the particulate fluxes of organic carbon and of phosphorus were in agreement with measurements (cf. Section 5.2). In order to achieve these results, a variable stoichiometry of primary production with respect to phosphate was necessary, so that the phosphorus content of newly built algae can decrease when phosphate gets limited. Moreover, consideration of a phosphate uptake process on sinking particles below the photic zone was necessary (cf. Section 5.4). The predictions of the model to the years after the calibration period were also very close to the measurements. This is not as astonishing as it may seem, because the external driving conditions and therefore also the seasonal pattern of concentrations did not significantly change during this time.

In contrast to the good general agreement of model with measurements, the model was not able to describe occasionally occurring blooms of specific species of algae. This cannot be avoided with a model of this degree of aggregation. Note, that even much more detailed phytoplankton models fail at the species level and give only adequate results on a more aggregated level than is used in the model description (Elliott et al., 2000).

The model was used to calculate conversion rates of oxygen, nitrate and phosphate that are not directly measured (cf. Section 5.3). These results are very useful for understanding the relative significance of different processes in the model and, with the aid of additional, more specific measurements, to improve our understanding of nutrient dynamics in the lake.

Although the model results look very promising, further applications of the model to different periods of Lake Zürich and to other lakes are necessary to improve the predictive capabilities of the model also for situations with significant changes in driving conditions.

Acknowledgements

We thank Sonja Gammeter and Ulrich Zimmerman from Wasserversorgung Zürich, Switzerland, Cohn Reynolds from Windermere Laboratory, Ambleside, United Kingdom, and

Table 5
Physical parameters used in the lake model

Parameter	Value	Ref.	Parameter	Value	Ref.
H_{sed}	0.0036 m	Eqs. (1), (3)–(6)	$v_{sed,ORG}$	10 md^{-1}	Eqs. (2), (5) and (7)
k_1	0.31 m^{-1}	Eq. (9)	$v_{sed,PLR}$	0 md−1	Eqs. (2), (5) and (7)
k_2	0.026 gWM^{-1} m^2	Eq. (9)	$v_{sed,ZOO}$	0 md^{-1}	Eqs. (2), (5) and (7)
$v_{O2,atm}$	1 m d^{-1}	Section 4.3	θ	0.95	Eqs. (3) and (4)
$v_{sed,ALG}$	0.2 m d^{-1}	Eqs. (2), (5) and (7)			

Table 6
Stoichiometric parameters used in the lake model

Parameter	Value	Ref.	Parameter	Value	Ref.
a_N	0.063	Tables 2 and 3	$S_{HPO4,crit}$	0.0042 gPm^{-3}	Table 3
$a_{P,max}$	0.009	Table 4	w_{ALG}	5	Section 2.2
$a_{P,red}$	0.0087	Tables 2 and 3	w_{ORG}	5	Section 2.2
$b_{P,min}$	0.0014	Table 3	w_{ZOO}	5	Section 2.2
$b_{P,max}$	0.0087	Table 3	$Y_{ZOO,max}$	0.5	Table 3
c_e	0.7	Table 3	ΔS_{HPO4}	0.0013 gPm^{-3}	Table 3
f_p	0.1	Table 2			

Table 7
Kinetic parameters used in the lake model

Parameter	Value	Ref.	Parameter	Value	Ref.
k_{death,ALG,T_0}	0.03 d^{-1}	Table 4	$K_{I,ALG}$	34 Wm^{-2}	Table 4
k_{death,PLR,T_0}	0.03 d^{-1}	Table 4	$K_{I,PLR}$	2 Wm^{-2}	Table 4
k_{death,ZOO,T_0}	0.029 d^{-1}	Table 4	$K_{NH4,nitri}$	0.5 gNm^{-3}	Table 4
k_{gro,ALG,T_0}	1.1 d^{-1}	Table 4	$K_{NO3,ALG}$	0.04 gNm^{-3}	Table 4
k_{gro,PLR,T_0}	0.13 d^{-1}	Table 4	$K_{NO3,miner}$	0.1 gNm^{-3}	Table 4
k_{gro,ZOO,T_0}	0.30 $gDM^{-1}m^3d^{-1}$	Table 4	$K_{O2,upt}$	0.5 gOm^{-3}	Table 4
$k_{miner,aero,sed,T_0}$	0.1 d^{-1}	Table 4	$K_{O2,miner}$	0.2 gOm^{-3}	Table 4
$k_{miner,aero,wat,T_0}$	0.01 d^{-1}	Table 4	$K_{O2,nitr}$	0.4 gOm^{-3}	Table 4
$k_{miner,anox,sed,T_0}$	0.1 d^{-1}	Table 4	$K_{O2,resp}$	0.5 gOm^{-3}	Table 4
$k_{miner,anox,wat,T_0}$	0.01 d^{-1}	Table 4	$K_{HPO4,ALG}$	0.0019 gPm^{-3}	Table 4
k_{nitri,sed,T_0}	0.5 $gNm^{-3}d^{-1}$	Table 4			
k_{nitri,wat,T_0}	0.1 $gNm^{-3}d^{-1}$	Table 4	β_{ALG}	0.046°C^{-1}	Table 4
k_{resp,ALG,T_0}	0.05 d^{-1}	Table 4	β_{BAC}	0.046°C^{-1}	Table 4
k_{resp,PLR,T_0}	0.01 d^{-1}	Table 4	β_{PLR}	0.046°C^{-1}	Table 4
k_{resp,ZOO,T_0}	0.003d^{-1}	Table 4	β_{ZOO}	0.08°C^{-1}	Table 4
k_{upt}	1200 $gDM^{-1}m^4d^{-1}$	Table 4			

Hans Rudolf Bürgi, Maria Dittrich, René Gächter, Gerrit Goudsmit, Dieter Imboden, Frank Peeters, Laura Sigg, Bernhard Wehrli and Alfred Wüest from EAWAG, Switzerland, for many helpful discussions and comments. The local water supply authority (Wasserversorgung Zürich, WVZ), the local water protection authority (Amt fur Gewässerschutz und Wasserbau, AGW), the Swiss Meteorological Institute (SMA) and the Swiss Federal Institute for Environmental Science and Technology (EAWAG) kindly provided data used for this study.

Appendix A

This appendix contains the values of the model parameters used for the final simulation shown in this paper. For each parameter, value and unit is given, and, instead of a verbal description, a reference to the section, equation or table, where its meaning can be found. A summary of the origin of the parameter values is given in the text.

In addition to the parameters given in this appendix, initial values of state variables and time series for external variables (inflows, light at the water surface, water temperature, diffusivities) had to be provided in order to be able to perform a simulation. The origin of these data is discussed in Section 2.2.

Table 5 contains the values of the physical model parameters. Due to the very rough discretization of the sediment, the thickness of the two sediment layers, h_{sed}, is an empirical parameter, which was fitted. The values of the light extinction parameters, k_1 and k_2 were fitted independently of the model on raw data from WVZ. The value of the oxygen exchange velocity, $V_{\text{O2,atm}}$, was selected to be in the range used for other lake simulations in Switzerland (Imboden and Gächter, 1978; Karagounis et al., 1993). Finally, information on sedimentation velocity was gained from Imboden and Gächter (1978), Karagounis et al. (1993), Andersen (1997), Lampert and Sommer (1997).

Table 6 contains the values of the stoichiometric model parameters. Basic nitrogen and phosphorus fractions, a_{N} and $a_{\text{P,red}}$, were based on the mass composition according to Redfield et al. (1966). Information on $a_{\text{P,max}}$ came from Sigg et al. (1987) and Hupfer et al. (1995). The parameters for variable phosphorus stoichiometry, $b_{\text{P,min}}$ and $b_{\text{P,max}}$ were selected using Hupfer et al. (1995), Andersen (1997). The parameter c_{e} was adjusted during preliminary simulations. The mass fraction of inert organic matter during death processes, f_{p} was selected to have a similar value as in activated sludge sewage treatment models (Henze et al., 1986). The critical value for switching from Redfield stoichiometry to reduced phosphorus stoichiometry, $S_{\text{HPO4,crit}}$, was fitted. The selection of the ΔS_{HPO4} was influenced by the fitted value of $S_{\text{HPO4,crit}}$ and by personal discussions with Reynolds. Finally, the values of the conversion factors between dry mass and wet mass, w, and the maximum yield of zooplankton, $Y_{\text{ZOO,max}}$, was selected using Andersen (1997) and personal information from Reynolds.

Table 7 contains the values of the kinetic model parameters. The parameters k, in the left column, are maximum conversion rates at $T_0 = 20°\text{C}$, the parameters K, in the right column, are half-saturation concentrations, and the parameters β, in the right column, are temperature dependence coefficients. Information on the values of these parameters came from many different sources. The parameters $k_{\text{death,ZOO},T_0}$, $k_{\text{gro,ALG},T_0}$, $k_{\text{gro,ZOO},T_0}$, $K_{\text{I,ALG}}$ and $K_{\text{HPO4,ALG}}$ were fitted (cf. Omlin et al. (2001) for details of fit parameter selection). The parameters for *Oscillatora rubescens* growth, $k_{\text{death,PLR},T_0}$ $k_{\text{gro,PLR},T_0}$ $k_{\text{resp,PLR},T_0}$ and $K_{\text{I,PLR}}$ were adjusted manually due to problems with the sharp peaks in the fit. Information on other kinetic parameters came from Imboden and Gächter (1978), Karagounis et al. (1993), Cooper (1984), Henze et al. (1986), Andersen (1997), Lampert and Sommer (1997). Temperature dependence for algae and bacteria was taken from Brown and Barnwell (1987) and for zooplankton from personal communication with H.R. Bürgi.

References

AGW, 1985. Studie über den Phosphoreintrag in den Zürichsee aus natürlichen Zuflüssen. Amt für Gewässerschutz und Wasserbau (AGW), Zürich, Switzerland.

AGW, 1992. Oberflächengewasser und Kläranlagen. Amt für Gewässerschutz und Wasserbau (AGW), Zürich, Switzerland.

Andersen, T., 1997. Pelagic Nutrient Cycles. Berlin, Springer.

Andersen, T., Hessen, D.O., 1991. Carbon, nitrogen and phosphorus content of freshwater zooplankton. Limnology Oceanography 36, 807–814.

Belsley, D.A., 1991. Conditioning Diagnostics — Collinearity and Weak Data in Regression. Wiley, New York.

Belsley, D.A., Kuh, E., Welsch, R.E., 1980. Regression Diagnostics — Identifying Influential Data and Sources of Collinearity. Wiley, New York.

Brown, L.C., T.O. Barnwell, 1987. The enhanced stream water quality models QUAL2E and QUAL2E-UNCAS: Documentation and user manual. Technical report, Environmental Research Laboratory Office of Research and Development, US Environmental Protection Agency, Athens, GA.

Brun, R., Reichert, P., Künsch, H.-R., 2001. Practical identifiability analysis of large environmental simulation models. Water Resources Research 37 (4), 1015–1030.

Cole, T.M., Buchak, E., 1995. CE-QUAL-W2: A two-dimensional, laterally averaged, hydrodynamic and water quality model, version 2.0. Technical report, US Army Corps of Engineers Waterways Experiments Station, Vicksburgh, MS.

Cole, T.M., Wells, S.A., 2000. CE-QUAL-W2: A two-dimensional, laterally averaged, hydrodynamic and water quality model, version 3.0. Technical report, US Army Engineering and Research Development Center, Vicksburgh, MS.

Cooper, B., 1984. Activities of bentic nitrifiers in streams and their role in oxygen consumption. Microbial Ecol. 10 (2), 191–198.

De Groot, W., 1983. Modelling the multiple nutrient limitation of algal growth. Ecol. Modell. 18, 99–119.

Droop, M., 1983. 25 years of algal growth kinetics. Botanica Marina XXVI, 99-112.

EAWAG, 1992. Einleitungskonzept Zürichsee. Zusammenfassung. Dübendorf, Switzerland: EAWAG. Bericht zuhanden des Amtes für Gewässerschutz und Wasserbau des Kantons Zürich.

Elliott, J.A., Irish, A.E., Reynolds, C.S., Tett, P., 1999a. Sensitivity analysis of PROTECH, a new approach in phytoplankton modelling. Hydrobiologia 414, 45–51.

Elliott, J.A., Reynolds, C.S., Irish, A.E., Tett, P., 1999b. Exploring the potential of the PROTECH model to investigate phytoplankton community theory. Hydrobiologia 414, 37–43.

Elliott, J.A., Reynolds, C.S., Irish, A.E., Tett, P., 2000. Modelling freshwater phytoplankton communities: an exercise in validation. Ecol. Modell. 128, 19–26.

Elser, J.J., Hassett, R.P., 1994. A stoichiometric analysis of the zooplankton–phytoplankton interaction in marine and freshwater ecosystems. Nature 370, 211–213.

Ford, D.E., Stefan, H., 1980. Thermal prediction using integral energy model. J. Hydraulic Eng. Division ASCE 106, 39–55.

Gächter, R., Mares, T., 1985. Does settling seston release soluble reactive phosphorus in the hypolimnion of lakes? Limnology Oceanography 30, 364–371.

Gammeter, S., Forster, R., Zimmerman, U., 1997. Limnologische Untersuchung des Zürichsees 1972–1996. Technical report, Wasserversorgung Zürich, Qualitätsüberwachung.

Gear, C.W., 1971. The automatic integration of ordinary differential equations. Cornmun. ACM 1 (3), 176–179.

Gujer, W., Henze, M., Mino, T., Matsuo, T., Wentzel, M.C., Marais, G.v.R., 1995. The activated sludge model no. 2: Biological phosphorus removal. Water Sci. Technol. 31 (2), 1–11.

Hamilton, D.P., Schladow, S.G., 1997. Prediction of water quality in lakes and reservoirs. Part 1 — Model description. Ecol. Modell. 96, 91–110.

Henze, M., Grady, C.P.L., Gujer, W., Marais, G. v. R., Matsuo, T., 1986. Activated sludge model no. 1. Scientific and Technical Report 1, IAWPRC Task Group on Mathematical Modelling for Design and Operation of Biological Wastewater Treatment Processes, IAWPRC, London.

Hessen, D., 1992. Nutrient element limitation of zooplankton production. Am. Nat. 140, 799–814.

Hupfer, M., Gächter, R., Giovanoli, R., 1995. Transformation of phosphorus species in settling seston and during early sediment diagenesis. Aquat. Sci. 57, 305–324.

Imberger, J., Patterson, J.C., 1981. A dynamic reservoir simulation model — DYRESM. In: Fischer, H.B. (Ed.), Transport models for inland and coastal waters. Academic Press, New York, pp. 310–361.

Imboden, D.M., Gächter, R., 1978. A dynamic lake model for trophic state prediction. Ecol. Modell. 4, 77–98.

Karagounis, I., Trösch, J., Zamboni, F., 1993. A coupled physical-biochemical lake model for forecasting water quality. Aquat. Sci. 55 (2), 87–102.

Ketchum, B., 1939. The absorption of phosphate and nitrate by illuminated cultures of Nitzschia closterium. Am. J. Bot. 26, 399–407.

Lampert, W., Sommer, U., 1997. Limnoecology. Oxford University Press.

Li, Y., 1973. Eddy diffusion in lake Zürich. Hydrologie 35, 1–7.

McQueen, D.J., Post, J.R., Mills, E.L., 1986. Trophic relationships in freshwater pelagic ecosystems. Can. J. Fish. Aquat. Sci. 43, 1571–1581.

Mengis, M., Gächter, R., Wehrli, B., 1997. Nitrogen elimination in two deep eutrophic lakes. Limnology Oceanography 42, 1530–1543.

Nelder, J.A., Mead, R., 1965. A simplex method for function minimization. Comput. J. 7, 308–313.

Omlin, M., Brun, P., Reichert, P., 2001. Biogeochemical model of Lake Zürich: Sensitivity, identifiability and uncertainty analysis. Ecol. Modell. 141, 105–123.

Pace, M., 1984. Zooplankton community structure but not biomass, influences the phosphorus-chlorophyll a relationship. Can. J. Fish. Aquat. Sci. 41, 1089–1096.

Petzold, L., 1983. A description of DASSL: A differential/algebraic system solver. In: Stepleman, R.E. (Ed.), Scientific Computing. IMACS/North-Holland, Amsterdam, pp. 65–68.

Powell, T., Jassby, A., 1974. The estimation of vertical eddy diffusivities below the thermocline in lakes. Water Resources Res. 10 (2), 191–198.

Ralston, M.L., Jennrich, R.I., 1978. DUD-a derivative-free algorithm for nonlinear least squares. Technometrics 20 (1), 7–14.

Redfield, A.C., Ketchum, B., Richars, F., 1966. The influence of organism on the composition of seawater. In: Hill, M. (Ed.), The Sea, vol. 2. Wiley Interscience, New York.

Reichert, P., 1994. AQUASIM — A tool for simulation and data analysis of aquatic systems. Water Sci. Technol. 30 (2), 21–30.

Reichert, P., 1998. AQUASIM 2.0 — User Manual. Technical report, Swiss Federal Institute for Environmental Science and Technology (EAWAG), Dubendorf, Switzerland.

Reichert, P., Borchardt, D., Henze, M., Rauch, W., Shanahan, P., Somlyódy, L., Vanrolleghem, P., 2001. River water quality model no. 1 (RWQM1): II. Biochemical process equations. Water Sci. Technol. 43 (5), 11–30.

Reynolds, C.S., 1997. Vegetation Processes in the Pelagic: A Model for Ecosystem Theory. Ecology Institute, Oldendorf/Luhe.

Reynolds, C.S., Irish, A.E., 1997. Modelling phytoplankton dynamics in lakes and reservoirs: the problem of in-situ growth rates. Hydrobiologia 39, 5–17.

Riley, M.J., Stefan, H.G., 1988. MINLAKE: A dynamic lake water quality simulation model. Ecol. Modell. 43, 155–182.

Schladow, S.G., Hamilton, D.P., 1997. Prediction of water quality in lakes and reservoirs. Part ii-Model calibration, sensitivity analysis and application. Ecol. Modell. 96, 111–123.

Shanahan, P., Borchardt, D., Henze, M., Rauch, W., Reichert, P., Somlyódy, L., 2001. River water quality model no.1 (RWQM1): I. Modelling approach. Water Sci. Technol. 43 (5), 1–10.

Sigg, L., Sturm, M., Kistler, D., 1987. Vertical transport of heavy metals in settling particles in lake Zürich. Limnology Oceanography 32 (1), 112–130.

Sommer, U., 1991. Phosphorus-limited Daphnia: Intraspecific facilitation instead of competition. Limnology Oceanography 37, 966–973.

Steele, J., 1962. Environmental control of photosynthesis in the sea. Limnology Oceanography 7, 137–150.

Urabe, J., Watanabe, Y., 1992. Possibility of N or P limitation for planktonic cladocerans: An experimental test. Limnology Oceanography 37, 244–251.

Vanrolleghem, P., Borchardt, D., Henze, M., Ranch, W., Reichert, P., Shanahan, P., Somlyódy, L., 2001. River water quality model no.1 (RWQM1): III. Biochemical submodel selection. Water Sci. Technol. 43 (5), 31–40.

Wüest, A., 1987. Ursprung und Grösse von Mischungsprozessen im hypolimnion natürlicher Seen. PhD dissertation no. 8350, ETH Zürich, Zürich, Switzerland.

Wüest, A., Piepke, G., Van Senden, D.C., 2000. Turbulent kinetic energy balance as a tool for estimating vertical diffusivity in wind-forced stratified waters. Limnology Oceanography 45, 1388–1400.